Composite Structures 334 (2024) 117965

Contents lists available at ScienceDirect

Composite Structures

journal homepage: www.elsevier.com/locate/compstruct

Long-term creep behavior of novel self-anchored CFRP cable system

Pengcheng Ai [a,b], Guozhen Ding [a,c], Zhiyuan Li [a], Peng Feng [a,*]

[a] Key Laboratory of Civil Engineering Safety and Durability of China Education Ministry, Department of Civil Engineering, Tsinghua University, Beijing 100084, China
[b] The Fifth Scientific Research Institute of Wuxi, Wuxi 214035, China
[c] Department of Civil and Environmental Engineering, Imperial College London, London SW7 2AZ, UK

ARTICLE INFO

Keywords:
Carbon fiber-reinforced polymer (CFRP)
Cable
Anchorage
Creep
Relaxation
Residual mechanical properties

ABSTRACT

Carbon fiber-reinforced polymer (CFRP) cables are an attractive material for bridge cables due to their light weight, high strength, and corrosion resistance properties. However, research on their long-term creep performance is limited. In this study, long-term creep tests were conducted on self-anchored CFRP cables under various stress levels to evaluate their creep performance and residual mechanical properties. Based on experimental data, million-hour creep coefficients and relaxation coefficients were predicted. The results indicated that the self-anchored CFRP cable system had a million-hour creep coefficient ranging from 6.1 % to 7.9 % at stress levels from 0.3 f_u to 0.7 f_u (where f_u represents the characteristic tensile strength). Additionally, maintaining low and medium stress levels for 1000 h improved the tensile strength and stability of the CFRP cables. The self-anchored CFRP system was also able to provide effective anchorage even after continuous loading. By comparing with the steel cable data in the literature, the self-anchored CFRP system exhibited smaller creep and relaxation, as well as superior residual tensile properties. These findings suggested that the self-anchored CFRP cable exhibited favorable long-term reliability, and finally self-anchored CFRP cables were successfully applied to a bridge in the campus of Tsinghua University.

1. Introduction

Carbon fiber-reinforced polymer (CFRP) has emerged as a promising material for cable applications in structures given its advantageous properties such as high strength-to-weight ratio, corrosion resistance, and fatigue resistance [1–5]. However, as an anisotropic material, the transverse compressive strength and shear strength of CFRPs are considerably less than the longitudinal tensile strength, posing a challenge for its effective anchoring in engineering applications [6]. To address the aforementioned issue, researchers have proposed various anchoring methods primarily utilizing surface force transmission mechanisms such as mechanical friction or bonding forces [6]. However, due to the lower shear strength of CFRP, the anchoring efficiency of these methods is typically limited. Therefore, we have introduced a novel self-anchored CFRP cable system [2–4,7], as shown in Fig. 1. In this system, CFRP is wound around the anchoring area, allowing CFRP to primarily experience tensile loading and possessing a straightforward and efficient anchoring mechanism. The cable system comprises two variations based on cable length: the combined type and the integrated type. The combined type consists of two distinct components, namely the anchorages and the cable body. These components can be connected using pre-clamp lap joints [2,3], resulting in an assembled CFRP cable with a relatively substantial length. The key advantage of this type of CFRP cable lies in the ability to prefabricate both the anchorages and the cable body in a factory setting, subsequently assembling them at the construction site. This approach significantly simplifies the transportation and installation of CFRP cables. On the other hand, the integrated type is designed as a readily available product with a cable length suitable for transportation. By utilizing the continuous winding technique, the anchorages and the cable body are simultaneously formed, eliminating the need for any joints between them. The novel self-anchored CFRP cable system offers numerous advantages, including high anchoring efficiency, a lightweight design, and easy installation. However, it is crucial to investigate the long-term creep behavior of the self-anchored CFRP cable under sustained loading, as it has the potential to impact the stability and safety of the entire structure [8,9].

The creep development in fiber-reinforced polymers (FRP) is a crucial behavior that has been investigated in previous studies. In this regard, the creep process can be characterized by three different stages [10], as demonstrated in Fig. 2. The primary creep stage is characterized

* Corresponding author at: Department of Civil Engineering, Tsinghua University, Beijing 10084, China.
E-mail addresses: g.ding23@imperial.ac.uk (G. Ding), lizhiyua18@mails.tsinghua.edu.cn (Z. Li), fengpeng@tsinghua.edu.cn (P. Feng).

https://doi.org/10.1016/j.compstruct.2024.117965
Received 28 September 2023; Received in revised form 25 December 2023; Accepted 6 February 2024
Available online 9 February 2024
0263-8223/

by a rapid increase in creep strain followed by a gradual reduction in the growth rate until it reaches a steady state. The secondary creep stage may persist for an extended duration during which the creep behavior remains relatively constant, as shown by the green line in Fig. 2. However, at higher stress levels, the material may undergo a transition to the third stage, known as tertiary creep, where the creep strain increases rapidly, leading to material failure through creep rupture, as shown by the orange line in Fig. 2. In cases of very high stress levels, creep rupture can occur during the first stage, as shown by the red line in Fig. 2. Thus, comprehending the different stages of creep development is crucial for predicting the long-term behavior of composite materials subjected to sustained loading conditions.

The investigation of creep behavior in various types of FRP materials under different environmental conditions and stress levels has been extensively researched. These studies have mainly focused on three aspects: creep coefficient, creep rupture strength, and residual properties. Specifically, the creep coefficient is defined as the ratio of creep strain to initial strain, with lower values indicating better creep performance. Creep rupture strength is defined as the maximum continuous load level that a material or structure can sustain throughout its service life without undergoing creep rupture. For span bridges, which are typically designed to last for 100 years, it is common practice to calculate the creep rupture strength with a load holding time of 114 years (10^6 h) to ensure adequate safety [12]. Residual properties describe the mechanical properties of a material after undergoing creep deformation.

To comprehend the development of creep behavior in materials, creep tests and theoretical models have been used to fit and predict the material creep coefficient. In 1992, Guimaraes and Burgoyne [13] conducted an experiment on the creep behavior of Parafil rope with aramid fiber, assessing its creep behavior at ambient temperature for up to 580 days. The results indicated that the creep and recovery of the Parafil rope could be described by a logarithmic relationship with time, and there was no significant correlation between the creep coefficient and the stress level. In 2003, Zou [14] performed a 1000-hour creep test on 8 mm-diameter aramid fiber-reinforced polymer (AFRP) bars at a stress level from 40 % to 70 % of the ultimate tensile strength. Based on the test results and logarithmic regression analysis, the predicted million-hour creep coefficient was 13.3 %. Banibayat and Patnaik [15] conducted a creep test on 4.3 mm-diameter basalt fiber-reinforced polymer (BFRP) bars with a stress level from 25 % to 80 % of the ultimate tensile strength, simulating environmental conditions in concrete

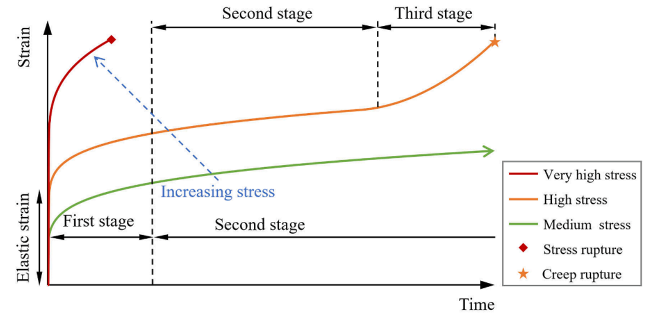

Fig. 2. Creep deformations over time (adapted from Ref. [11]).

using an alkaline solution and a high temperature (60℃) accelerated test. The results revealed that the predicted million-hour creep coefficient of the BFRP bars was 12.9 %, slightly less than that of the AFRP bars. Ascione et al. [16,17] conducted creep tests on glass fiber-reinforced polymer (GFRP) laminates and their constituent phases (fiber and matrix) under constant environmental conditions. They simulated the creep behavior of GFRP based on a four-parameter rheological mechanics model, assuming no slip between the matrix and fiber. The predictions of this model were in good agreement with the experimental results. This model explains the creep behavior mechanism of the composite: the different rheological properties of the matrix and fiber lead to stress transfer from the matrix to the fiber, the viscous deformation of the fiber is ignored, the stress of the matrix gradually approaches zero, and the axial strain of the composite eventually tends to have a constant value over time.

The testing methodology for evaluating creep rupture strength is outlined in ASTM D7337 [12], which involves subjecting FRP bars to different stress levels during the creep test and recording the corresponding stress level and time of failure. Linear regression analysis using the least squares method can establish a correlation between the logarithm of endurance time and creep rupture strength from the acquired test data. Wang et al. [18,19] conducted a 1000-hour creep test on 6 mm-diameter BFRP bars and found that the million-hour creep rupture strength was 52 % of the tensile strength with 95 % reliability. Pretension treatment led to enhanced creep performance of BFRP bars, resulting in a 17 % increase in their million-hour creep rupture strength. Furthermore, Benmokrane et al. [20] performed a statistical analysis of

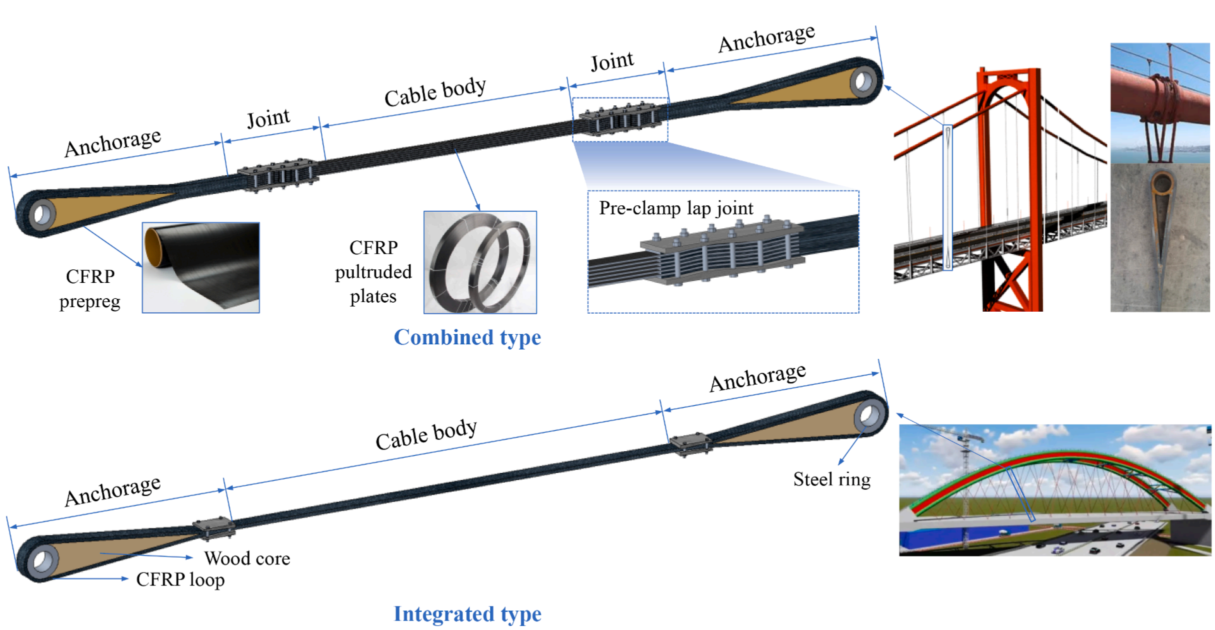

Fig. 1. Novel self-anchored CFRP cable system [2–4].

204 creep rupture tests across eight studies and determined that the million-hour creep rupture strength of GFRP bars was 50.7 % of the average ultimate tensile strength.

Researchers usually perform static tensile tests on materials that have not undergone creep rupture after conducting creep testing to assess the impact of creep on mechanical properties. Yang et al. [21] conducted high-stress creep tests on CFRP tendons with field-made anchorages for 3,624 h and observed that the residual strength of the CFRP tendons was significantly greater than their guaranteed strength, indicating good performance under very high stress levels. In another study, Yang et al. [22] noted that the residual strength of CFRP tendons decreased by 4.54 % after creep testing, while the residual elastic modulus increased by 6.99 %. Additionally, Jiang et al. [23] studied the creep behavior of CFRP cables at elevated temperatures, and their experimental results demonstrated that the degree of damage to the residual strength and elastic modulus of the cables increased with higher temperatures and stress levels.

A review of the literature on FRP composite creep behavior indicated that limited research was conducted on CFRP cable creep behavior, and there was a significant variation in the results of creep tests. Moreover, there are very few studies available on the creep behavior of self-anchored CFRP cables. Thus, this study aims to comprehensively investigate the creep behavior of self-anchored CFRP cables by analyzing their creep-time relationship under various stress levels, predicting creep and relaxation coefficients, and determining residual properties following 1000 h of sustained loading. Finally, this paper also presents the practical applications of self-anchored CFRP cables in engineering.

2. Experimental programs

2.1. Specimens

The self-anchored integrated CFRP cables used in the test consisted of two anchorages and a 200-mm-long cable body with a cross section of 25 mm × 1.2 mm, as shown in Fig. 3. The T70024S unidirectional carbon fiber prepreg material with a 36 % volume of epoxy resin was utilized to manufacture the CFRP loops and cable bodies through the continuous winding and vacuum bagging technique. C45E4 steel was used to make the steel rings, and poplar was used to make the wood core mold. Two steel plates and four bolts were used to prevent potential splitting failure in the transition area between the anchorage and cable body.

The layup method for the self-anchored CFRP cables is illustrated in Fig. 4. The specific steps are as follows: (a) Laying the first winding layer: The first layer of unidirectional carbon fiber prepreg is wound around the steel rings at two ends, with an overlap on one side of the cable body. The overlap length is no less than 200 times the thickness of the carbon fiber prepreg. (b) Laying the reinforcement layer: A layer of reinforcement is laid on the two anchoring regions. The reinforcement layer uses the same material as the winding layer (different colors are used for easy differentiation). (c) Laying the second winding layer: The second layer of unidirectional carbon fiber prepreg is wound around the cable body with an overlap on the other side. Then, a second layer of reinforcement is laid on the two anchoring regions. This cycle is repeated until the cable body and anchorages reach the designed thickness. (d) Vacuum curing: Place a flow mesh and flow tube on the laid carbon fiber prepregs, seal the specimen with sealing adhesive and a vacuum bag, and evacuate to maintain a pressure of 0.1 MPa. Place the sealed specimen in an oven, with an initial curing temperature of 110 °C and an initial curing time of 0.5 h, followed by a curing temperature of 140 °C and a curing time of 2 h. (e) Post-processing: After the specimen naturally cools, remove the vacuum bag, flow mesh, flow tube, release fabric, etc. Cut the specimen, and install steel plates in the transition area.

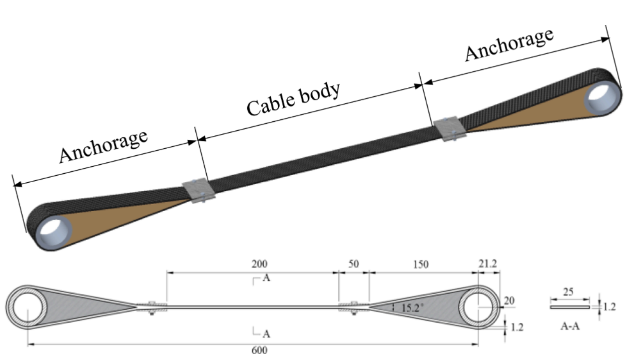

Fig. 3. Schematic of the self-anchored CFRP cables.

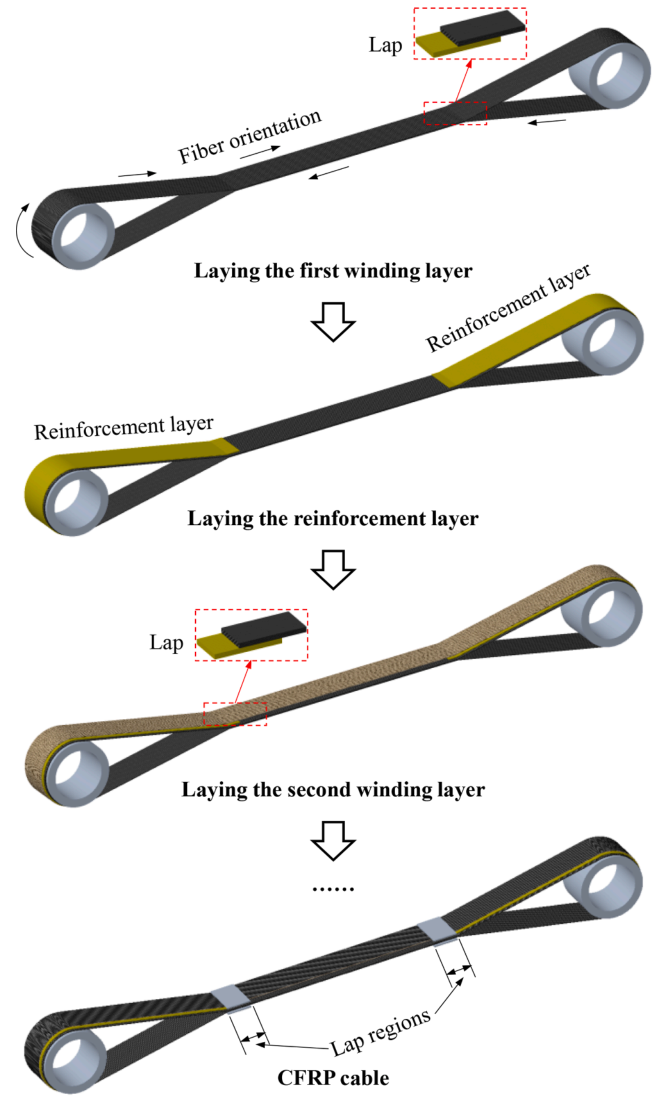

Fig. 4. Layup method for the self-anchored CFRP cables.

2.2. Short-term tensile test

To determine the ultimate tensile strengths and elastic modulus of self-anchored CFRP cables, short-term tensile tests were conducted using a hydraulic testing machine, as shown in Fig. 5. A tensile load was applied to the cables under displacement-controlled mode at a constant rate of 1 mm/min. The anchorage was connected with the fixture via a pin with an assembly gap of 0.4 mm between the pin and the steel ring.

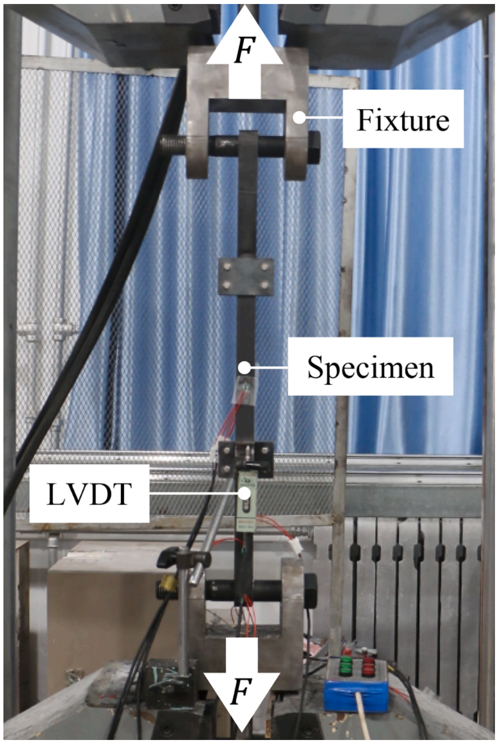

Fig. 5. Short-term tensile test setup.

Laser level alignment was performed during specimen installation to mitigate the impact of eccentricity during the test process. Prior to the tensile tests, specimens were pre-tensioned to a load of 5 % of their capacity to eliminate gaps between the specimen and fixture during installation and possible slip between the fixture and testing machine during the experiment.

2.3. Long-term creep test

A testing machine was made to ensure stable load application during the long-term creep test, as shown in Fig. 6. The lever principle was utilized to magnify the load of the counterweight and apply it to the CFRP cable at a factor of 7.65. The counterweight and the CFRP cable were installed on either side of the lever arm, with one end of the CFRP cable hinged on the lever arm and the other end hinged on the base through the reaction plate and bolts. The counterweight consisted of a steel basket weighing 70 kg and iron blocks, each weighing 20 kg [7]. Different quantities of iron weights were used to achieve the desired stress levels of the CFRP cables, which ranged from 0.3 to 0.7 f_u for 1000 h, as presented in Table 1. Here, "f_u" denotes the characteristic tensile strength of the CFRP cable.

To minimize the effect of external environmental and human factors, the creep test site was established in the basement of the Structural Laboratory at Tsinghua University. The site maintained an average ambient temperature of 18.5 °C, meeting the temperature requirements specified in JSCE-E533 (2004) [24]. According to the specifications, the test temperature should normally range within 20 ± 2 °C, while the average relative humidity should be maintained at 40 %.

To monitor the long-term creep strain of CFRP cables, Donghua 5G101 LVDTs (linear variable differential transformers) were employed with a measurement range of 10 mm, an accuracy of 0.005 mm, and a nonlinear error of ≤ 0.5 %. To collect data during the creep test, a Donghua DHDAS dynamic signal acquisition and analysis system was utilized with a data sampling frequency of 1 Hz.

Once the load was applied and stabilized, the displacements were reset to zero, and creep strain measurements began. The LVDT-1 determined the creep displacement of both the lower anchorage and cable body (s_1), while the LVDT-2 was responsible for measuring the creep displacement of the lower anchorage (s_2). As the cable body length (l) was 200 mm, the creep strain of the CFRP cable body could be calculated using the following equation:

$$\varepsilon_c = \frac{s_1 - s_2}{l} \quad (1)$$

3. Results

3.1. Short-term tensile properties

The results of short-term tensile tests for the self-anchored CFRP cables are presented in Table 2. In practical applications and the design of CFRP cables, it is important to consider the variation of their tensile strength. For this reason, the characteristic tensile strength (f_u = 2030.8 MPa) was used as the standard stress value in the creep test. The

Table 1
Creep test matrix.

Specimen ID	Temperature (°C)	Target stress level	Actual stress level	Creep time (h)
0.3 f_u	18.5 ± 0.5	30 %	30.2 %	1000
0.4 f_u	18.5 ± 0.5	40 %	39.9 %	1000
0.5 f_u	18.5 ± 0.5	50 %	49.6 %	1000
0.6 f_u	18.5 ± 0.5	60 %	59.3 %	1000
0.7 f_u	18.5 ± 0.5	70 %	71.3 %	1000

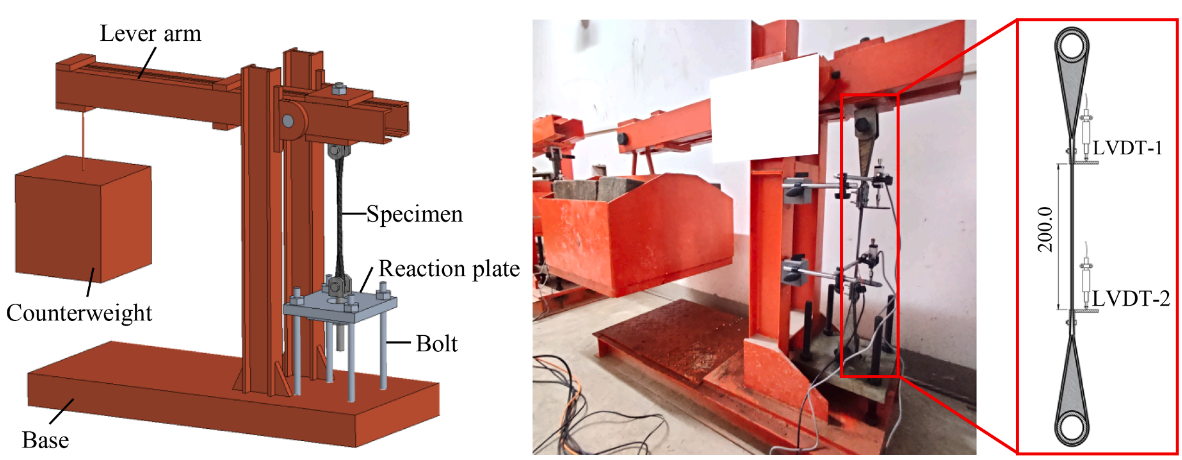

Fig. 6. Long-term creep test setup.

Table 2
Short-term tensile properties of the self-anchored CFRP cables.

Specimen	Tensile capacity (kN)	Tensile strength (MPa)	Elastic modulus (GPa)	Rupture strain (%)
S-1	64.9	2164.4	141.9	1.52
S-2	63.2	2106.5	137.2	1.53
S-3	72.1	2403.3	143.6	1.67
S-4	66.3	2211.5	140.1	1.58
S-5	69.7	2323.7	138.5	1.68
Mean value	67.2	2241.9	140.3	1.60
Standard deviation	3.2	107.7	2.3	0.07
Coefficient of variation	4.8 %	4.8 %	1.6 %	4.2 %
Characteristic value	–	2030.8	–	–

characteristic tensile strength corresponded to the 95th percentile of the strength distribution of the tested specimens, indicating that 95 % of the specimens demonstrated tensile strength greater than the characteristic value.

3.2. Long-term creep test results

Fig. 7 illustrates the creep and displacement curves of all specimens throughout the long-term creep test. The results indicated two distinct stages in the creep strain development of all specimens within the stress level range of 0.3 f_u ~ 0.7 f_u. During the first stage, the creep strain increased rapidly, while during the second stage, it gradually slowed with increasing time and stabilized at a slower creep rate. Notably, the first stage for all specimens did not exceed 120 h. The second stage lasted from 120 h to 1000 h and was characterized by a long-term and stable creep strain.

The creep coefficient is a fundamental parameter used to characterize the creep behavior of materials and represents the ratio of creep strain at a specific time to the initial strain. The creep coefficients for each specimen were computed at 72 h, 500 h, and 1000 h, as shown in Fig. 8. The results indicated that the creep coefficient increased with increasing duration of loading but showed no significant correlation with the stress level. This finding is consistent with the study by Guimaraes et al [13]. However, some research results suggested that the creep and relaxation of FRP increased with higher stress levels [22,25]. One possible explanation is that the creep coefficient of FRP remains relatively stable at moderate stress levels; however, beyond a certain threshold, the creep coefficient tends to rise with increasing stress levels. This phenomenon was observed in the experimental study conducted by Shi et al [26]. In our study, the maximum stress level was 0.7 f_u, whereas Yang et al [22] conducted creep tests under elevated stress levels ranging from 0.69 f_u to 0.85 f_u in their research. Consequently, no correlation between the creep coefficient and stress level was observed in our study, contrasting with the positive correlation noted by Yang et al [22]. It should be noted that this study only included one specimen for each stress level, and further experimental data are required to confirm this observation. The three curves in Fig. 8 exhibited similar undulating trends, indicating that higher short-term creep coefficients generally correspond to higher long-term creep coefficients. For the CFRP cables examined in this study, the creep coefficient ranged from 3.21 % to 4.31 % at 1000 h.

To gain further insight into the microscopic mechanism underlying the creep process of CFRP cables, specimens subjected to 0.5 f_u and 0.7 f_u were examined before and after the creep test using scanning electron microscopy (SEM), as presented in Fig. 9. The longitudinal section of the specimen before the creep test contained multiple uneven fibers. However, after the creep test, most of the fibers in the specimen subjected to 0.5 f_u appeared to be straightened. Similarly, for the specimen subjected to 0.7 f_u, most of the fibers were pulled straight, but some minor fiber breakage and interface cracks between the fiber and resin were observed. Based on the microscopic observations and analysis, it was concluded that initial fiber bending and interfacial defects between the fiber and resin are crucial factors that influence the creep rate and creep rupture strength of CFRP cables.

3.3. Creep coefficient prediction

To predict the long-term creep development of CFRP cables for 10^6 h (equivalent to 114 years), classical models have been employed to describe their creep behavior. The selection of an appropriate creep model is vital for accurately characterizing the creep of CFRP cables and predicting their long-term creep behavior. In this study, the Burgers model based on mechanics, the Findley model, and the logarithmic model based on empirical formulas were introduced to facilitate a comprehensive understanding of the creep performance of CFRP cables.

The Burgers model is a widely used rheological model that characterizes the relationship between stress, strain, and time through several basic elements [17], as shown in Fig. 10. Specifically, the elastic response is represented by a spring, while the viscous response is represented by a dashpot. The most common rheological models are the Maxwell model and the Kelvin model. The Maxwell model comprises a spring and dashpot in series, whereas the Kelvin model consists of a spring and dashpot in parallel. Although the Maxwell model can describe relaxation behavior to some extent, it is not suitable for effectively capturing creep behavior. Conversely, the Kelvin model is better suited for modeling creep behavior but falls short in capturing relaxation behavior. To overcome these limitations, the four-parameter Burgers model combines the Maxwell and Kelvin models in series, offering a more precise representation of viscoelastic behavior in composite materials with the ability to accurately capture both creep and relaxation behaviors [17].

The strain of the Burgers model can be divided into three components:

$$\varepsilon(t) = \varepsilon_{M1} + \varepsilon_{M2} + \varepsilon_K \tag{2}$$

where $\varepsilon(t)$ is the total strain in the creep process, ε_{M1} is the instantaneous elastic strain calculated by the spring element with an elastic modulus of E_M in the Maxwell model, ε_{M2} is the viscous strain calculated by the dashpot element with a viscosity coefficient of η_M, and ε_K is the delayed elastic strain calculated by the Kelvin model. The Kelvin model consists of a spring element with an elastic modulus of E_K and a dashpot element with a viscosity coefficient of η_K in parallel. Their relationships are given by the following equations:

$$\varepsilon_{M1} = \frac{\sigma_0}{E_M} \tag{3}$$

$$\varepsilon_{M2} = \frac{\sigma_0}{\eta_M} t \tag{4}$$

$$\varepsilon_K = \frac{\sigma_0}{E_K}\left(1 - e^{-\frac{E_K}{\eta_K}t}\right) \tag{5}$$

Therefore, the equation for total strain based on the Burgers model can be expressed as follows:

$$\varepsilon(t) = \sigma_0\left[\frac{1}{E_M} + \frac{t}{\eta_M} + \frac{1}{E_K}\left(1 - e^{-\frac{E_K}{\eta_K}t}\right)\right] \tag{6}$$

where σ_0 is the initial tensile stress and t is the load holding time. Its simplified form of this equation is:

$$\varepsilon(t) = a + bt + c\left(1 - e^{-dt}\right) \tag{7}$$

The Findley model is a power law model based on empirical formulas originally proposed by Findley in 1960 [27]. It has been used to characterize the creep behavior of viscoelastic materials [28]. The total strain equation based on the Findley model is given by:

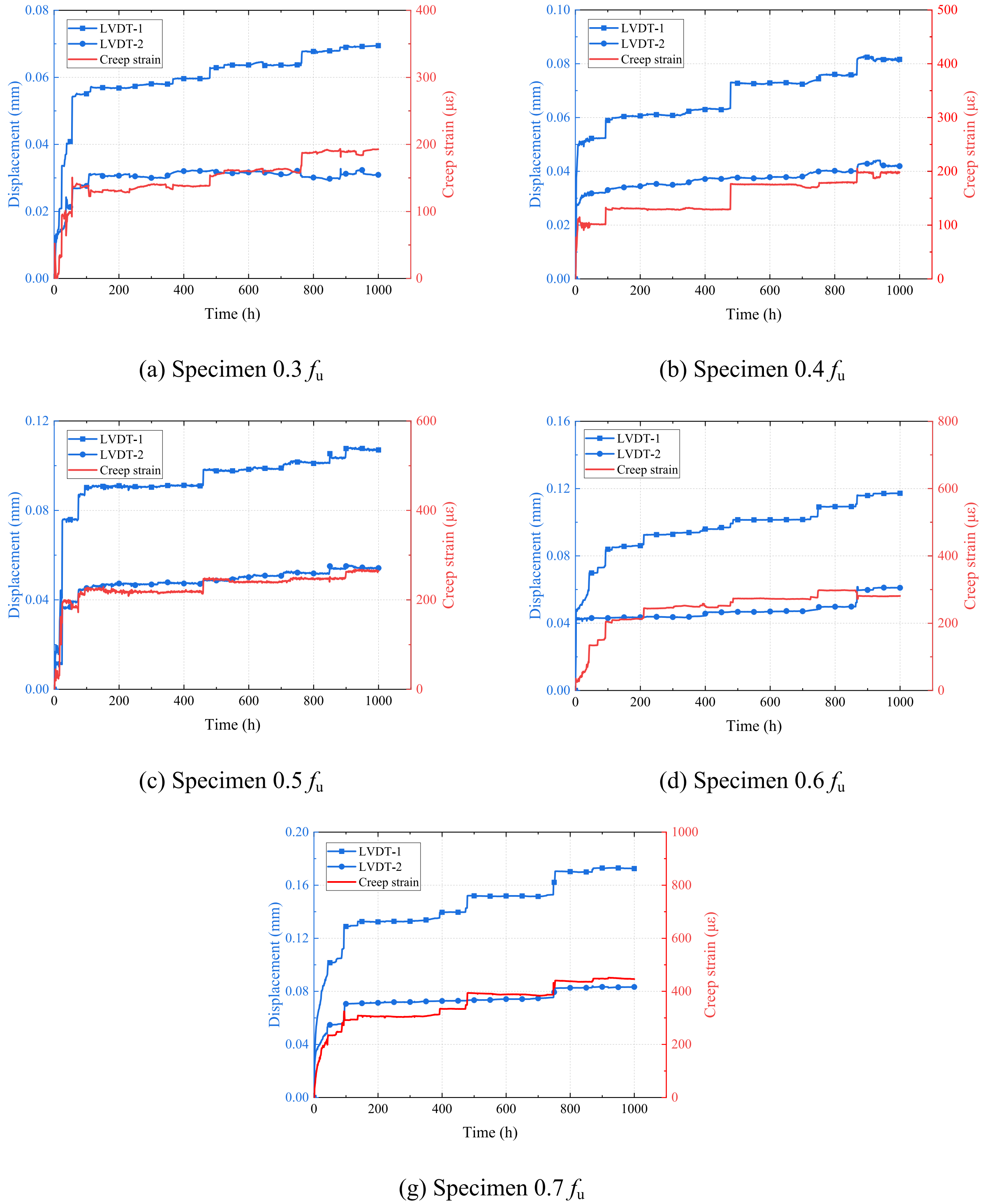

Fig. 7. Creep and displacement curves.

$$\varepsilon(t) = \varepsilon_0 + mt^n \tag{8}$$

where ε_0 is the initial elastic strain, m is the stress-dependent and temperature-dependent coefficient and n is the stress-independent material constant.

Research has shown that the tensile creep strain of FRP materials is linearly related to the logarithm of time [11,19,29]. Therefore, the total strain equation of the logarithmic model is given by:

$$\varepsilon(t) = \varepsilon_0 + a\ln t \tag{9}$$

where ε_0 is the initial elastic strain and a is a coefficient related to stress and material.

Yang et al. [22] used various creep models to fit the creep behavior of CFRP and found that the modified logarithmic law model provides better fitting accuracy. The total strain equation is given by:

$$\varepsilon(t) = \varepsilon_0 + a\ln t + bt \tag{10}$$

where ε_0 is the initial elastic strain and a and b are coefficients related to stress and material.

The above four creep models were used to fit the behavior of the

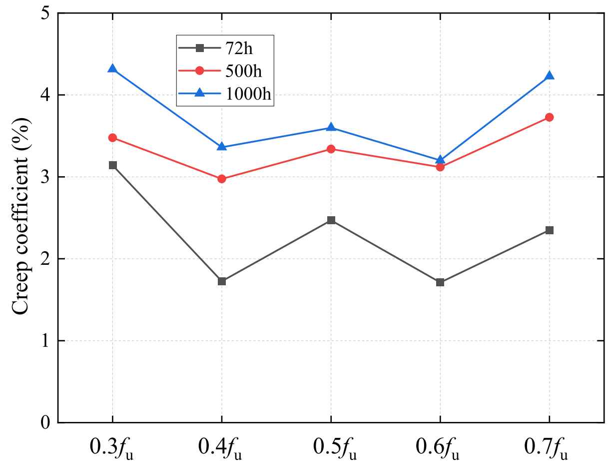

Fig. 8. Creep coefficient under different stress levels.

CFRP cables, as shown in Fig. 11. The fitting curves generated by the Burgers model and the modified logarithmic model exhibited a higher goodness of fit than the logarithmic model and Findley model. This suggests that the former models outperformed the latter in terms of fitting capability, primarily due to the greater number of parameters in the former models. However, it is important to note that the long-term creep prediction obtained from the Burgers model and modified logarithmic model approached a linear function of time for long-term creep prediction, resulting in a significant overestimation of creep values during later stages.

Given that CFRP cables are typically employed in long-span bridges with a design life of approximately 100 years, there is a need for creep data over 5×10^5 h (57 years) and 10^6 h (114 years). Table 3 shows the values of creep strain and creep coefficient predicted by each model under various stress levels. The results indicated that each model exhibited good short-term prediction accuracy, with similar predicted values for 1000 h. Nonetheless, the values predicted by the Burgers model and modified logarithmic model for 5×10^5 h and 10^6 h significantly exceeded the ultimate tensile strain of CFRP, which rendered their predicted values unreliable. For most stress levels, the predicted values of the creep coefficient of the Findley model for 10^6 h exceeded

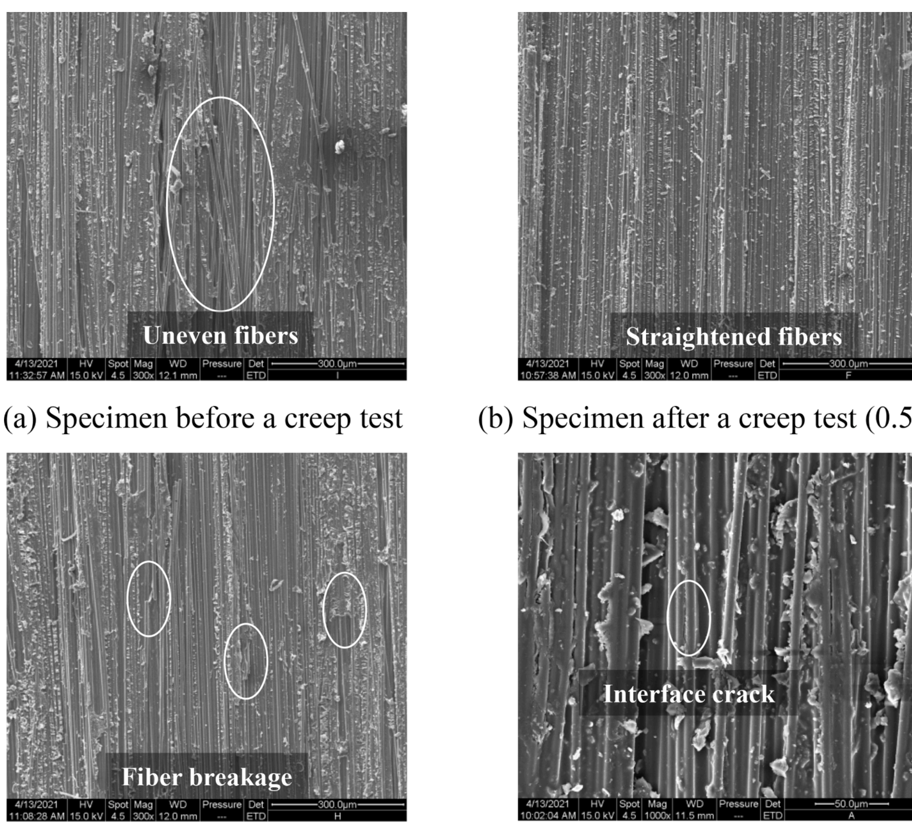

(a) Specimen before a creep test (b) Specimen after a creep test (0.5 f_u)

(c) Specimen after a creep test (0.7 f_u)

Fig. 9. SEM images of specimens.

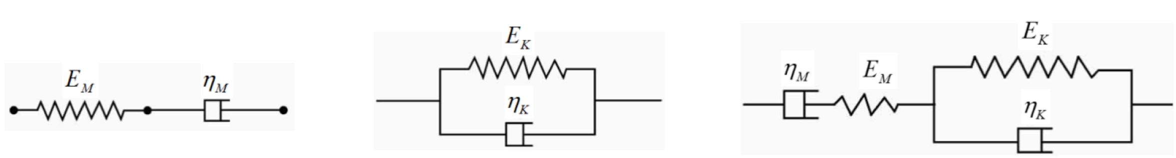

(a) Maxwell model (b) Kelvin model (c) Burgers model

Fig. 10. Rheological models.

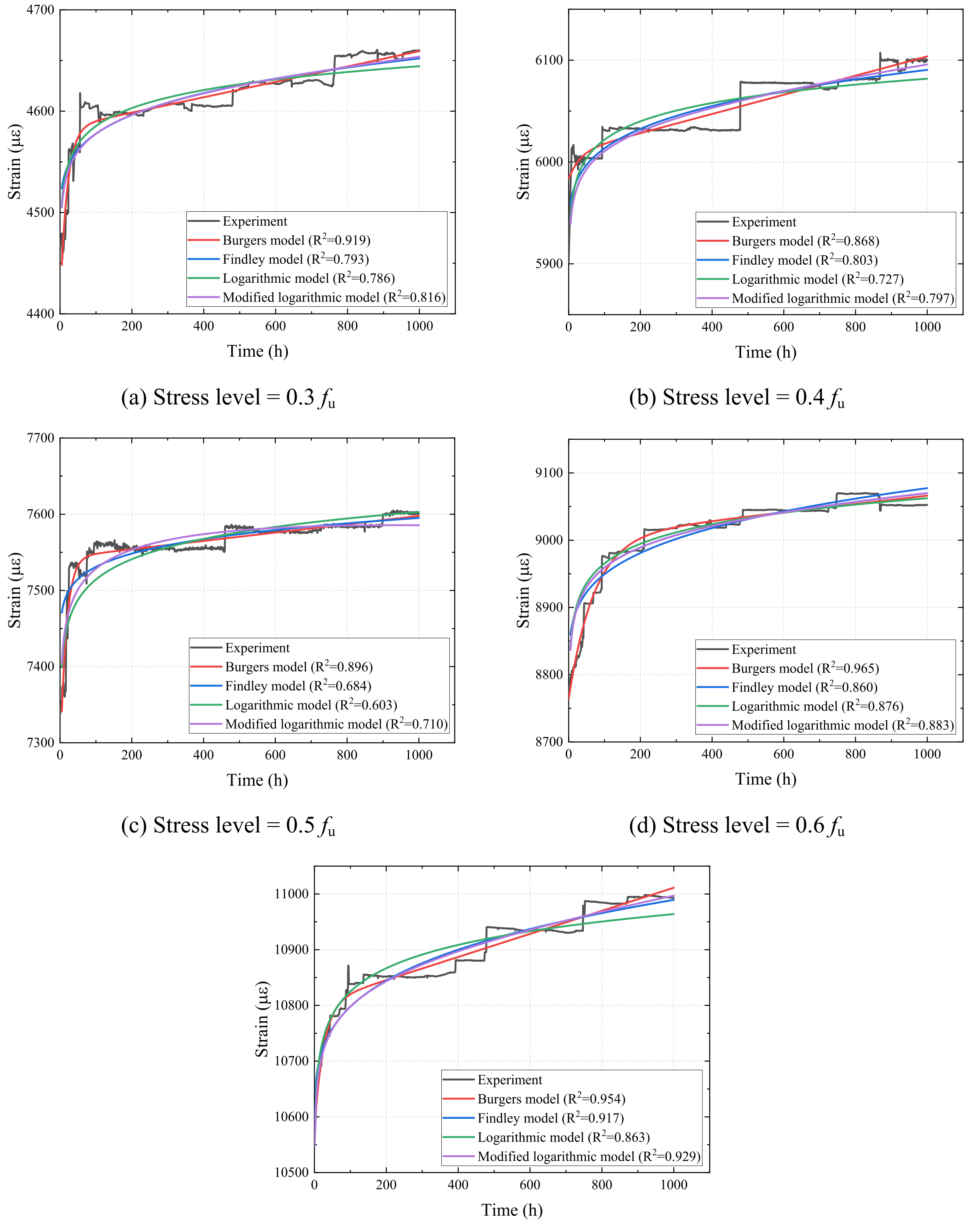

Fig. 11. The fitted curves of different models.

15 %, while the predicted values of the creep coefficient for 10^6 h under different stress levels of the logarithmic model were below 10 %.

Table 4 presents the predicted million-hour creep coefficients of various FRP materials from the literature. Most studies used the logarithmic model to fit and predict the creep behavior of FRP materials. For the AFRP material, the predicted million-hour creep coefficient ranged from 8.6 % to 14.3 %, while for the BFRP material, it ranged from 6.62 % to 12.9 %. In contrast, for the CFRP material, the predicted million-hour creep coefficient was smaller, ranging from 1.84 % to 3 %. In this study, the self-anchored CFRP cables were manually wound with prepreg, which lacked pre-tension during the production process. Therefore, the initial bending of fibers was more significant, resulting in a larger creep

Table 3
Predicted values of the creep strain and creep coefficient.

Stress level	Model	Creep strain (57 years)			Creep coefficient (%)		
		1000 h	5×10^5 h	10^6 h	1000 h	5×10^5 h	10^6 h
0.3 f_u	Burgers model	192.1	38116.1	76116.1	4.3	853.2	1703.9
	Findley model	184.9	736.9	860.2	4.1	16.5	19.2
	Logarithmic model	177.2	336.6	354.4	4.0	7.5	7.9
	Modified logarithmic model	186.6	12307.8	24324.1	4.2	275.5	544.5
0.4 f_u	Burgers model	201.5	47107.5	94107.5	3.4	798.1	1594.5
	Findley model	187.9	775.0	907.7	3.2	13.1	15.4
	Logarithmic model	179.7	341.4	359.5	3.0	5.8	6.1
	Modified logarithmic model	193.2	18298.6	36314.4	3.3	310.0	615.3
0.5 f_u	Burgers model	260.3	27206.3	54206.3	3.5	370.8	738.8
	Findley model	257.9	557.3	607.3	3.5	7.6	8.3
	Logarithmic model	266.2	505.6	532.3	3.6	6.9	7.2
	Modified logarithmic model	283.4	1036.4	1564.8	3.9	14.1	21.3
0.6 f_u	Burgers model	294.5	31232.5	62232.5	3.4	356.1	709.5
	Findley model	304.7	1312.6	1544.8	3.5	14.9	17.6
	Logarithmic model	290.7	552.2	581.4	3.3	6.3	6.6
	Modified logarithmic model	298.4	10528.8	20556.8	3.4	120.0	234.3
0.7 f_u	Burgers model	433.3	103726.3	207226.3	4.1	983.5	1964.8
	Findley model	441.4	2036.2	2414.8	4.2	19.3	22.9
	Logarithmic model	417.2	792.6	834.4	4.0	7.5	7.9
	Modified logarithmic model	450.0	43691.5	86728.1	4.3	414.3	822.3

Table 4
Comparison of the predicted million-hour creep coefficients.

Study	Material	Calculation formula	Predicted creep coefficient (10^6 h)
Guimaraes et al. (1992) [13]	AFRP	$\phi(t)$=(0.012 ± 0.0003) lg(t)	8.6 %~14.3 %
Zou (2003) [14]	AFRP	$\phi(t) = 0.0058\ \ln(t) + 0.0531$	13.3 %
Wang et al. (2016) [19]	BFRP	$\phi(t) = 0.0052\ \ln(t)$	6.62 %
Banibayat and Patnaik (2015) [15]	BFRP	$\phi(t) = 0.006\ \ln(t) + 0.0465$	12.9 %
Zou (2003) [14]	CFRP	–	≤3%
Yang et al. (2018) [22]	CFRP	$\phi(t) = 0.0012\ \ln(t) + 0.0025$	1.84 %~1.91 %
The present study	CFRP	$\phi(t) = 0.0057\ \ln(t)$	6.1 ~ 7.9 %

coefficient of the CFRP cables. The logarithmic model was more reasonable than the Findley model for predicting creep coefficients. As a result, the logarithmic model was chosen for subsequent creep coefficient calculations and stress relaxation coefficient predictions. According to the logarithmic model, the predicted million-hour creep coefficient for the self-anchored CFRP cables ranged from 6.1 % to 7.9 %.

3.4. Relaxation coefficient prediction

Creep and stress relaxation are two important behaviors that describe the time-dependent mechanical response of materials under different loading conditions. Creep refers to a gradual increase in strain over time while the material is subjected to a constant stress, whereas stress relaxation refers to a decrease in stress over time while the material is kept at a constant strain. These phenomena have a significant influence on the design and performance of materials in engineering applications. However, meeting the testing conditions for stress relaxation analysis stipulated by JSCE-E534 [24] is relatively demanding, and requires specialized equipment to eliminate anchorage slippage effects. To address this challenge, researchers such as Shi et al. [25] and Saadatmanesh et al. [30] developed specific equipment for stress relaxation testing. Alternatively, the behavior of stress relaxation can be deduced from creep testing data by establishing a relationship between creep and stress relaxation. Lakes and Vanderby [31] suggested that stress relaxation occurs due to the continuous transformation of elastic deformation into viscoelastic deformation over time, resulting in a gradual decrease in stress while the elastic modulus remains unchanged. During both stress relaxation and creep, viscoelastic deformation takes place continuously over time. Shi et al. [25] conducted creep and stress relaxation tests on BFRP bars, and the results confirmed the correlation between creep and stress relaxation via test data and stress–strain relationships. Their findings suggest that creep testing data can be used to simulate the stress relaxation behavior of FRP, potentially reducing the cost of stress relaxation testing.

Fig. 12 shows a typical stress relaxation curve and a creep curve. In stress relaxation, during a small-time increment Δt at time t, the stress is assumed to remain constant, and this period can be regarded as a creep process with a stress level of σ. During this process, creep strain ($\Delta\varepsilon_c$) occurs while the total strain remains constant, leading to a decrease in elastic strain and total stress. Thus, stress relaxation can be broken down into a series of creep processes where the stress level is gradually decreased over small periods.

For the process of stress relaxation, the total strain is composed of elastic strain and creep strain, and their relationship can be described by the following equation:

$$\varepsilon = \varepsilon_e + \varepsilon_c = \frac{\sigma}{E} + \varepsilon_c \tag{11}$$

where ε is the total strain, ε_e is the elastic strain, ε_c is the creep strain, σ is the total stress, and E is the elastic modulus.

Since the total strain is constant during stress relaxation, a differential equation can be derived as follows:

$$\dot{\varepsilon}_c = -\frac{1}{E}\dot{\sigma} \tag{12}$$

where $\dot{\varepsilon}_c$ is the creep rate of the stress relaxation process and $\dot{\sigma}$ is the stress relaxation rate.

The stress relaxation rate is proportional to the creep rate under the same stress level and load-holding time. With increasing load holding time, the stress retention decreases, and the creep rate also decreases. For the purpose of stress computation, the following iterative equation can be employed:

$$\sigma_n = \sigma_{n-1} - E\dot{\varepsilon}_c(\sigma_{n-1}, t_n)\Delta t \tag{13}$$

where σ_n is the stress of the nth iteration, σ_{n-1} is the stress of the (n-1)th iteration, and Δt is the time increment. The creep rate at the time t_n under stress level σ_{n-1} can be deduced using the logarithmic model.

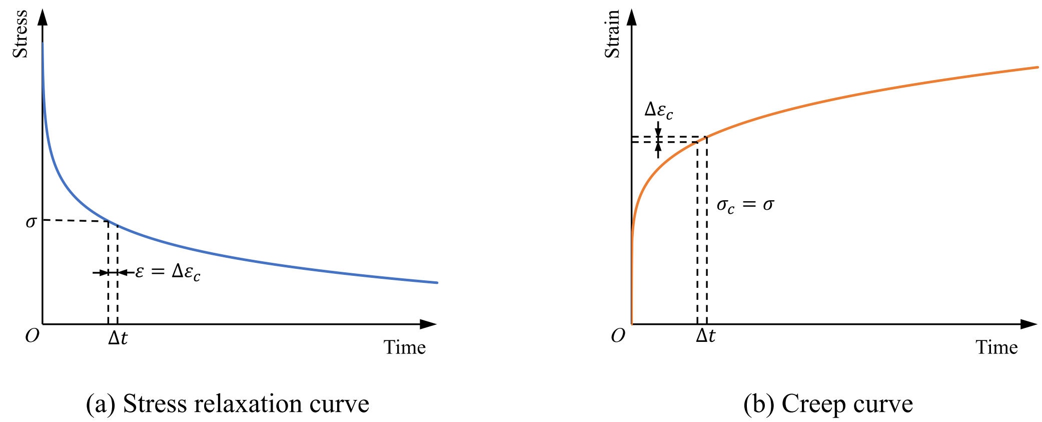

Fig. 12. Stress relaxation curve and creep curve.

Utilizing the logarithmic model for the creep process, stress relaxation curves under various initial stresses were derived through iterative calculations, as shown in Fig. 13. All stress relaxation curves demonstrated two stages. Stress levels exhibited a rapid decline during the first stage followed by a gradual deceleration. The initial stage of stress reduction was attributed to the straightening of initially bending fibers and the viscoelastic deformation of the resin. In the second stage, stress levels tended to stabilize. The magnitude of stress reduction resulting from stress relaxation was greater for higher initial stress levels. Table 5 shows the predicted stress retention and stress relaxation coefficients for different initial stress levels. The million-hour relaxation coefficient were 3.4 %, 3.7 %, and 5.0 % for initial stress levels of 0.5 f_u, 0.6 f_u, and 0.7 f_u, respectively. The findings suggested a positive correlation between the relaxation coefficient and the initial stress level, aligning with conclusions drawn in previous studies [25].

Table 6 lists the million-hour stress relaxation coefficients for different FRP materials predicted in various studies. The majority of the studies employed the logarithmic model to analyze and predict the stress relaxation behavior of FRP materials. However, the predicted outcomes differed considerably, which could be attributed to the differences in material characteristics chosen by the researchers, such as fiber type, resin content, and production process. For CFRP materials, the million-hour stress relaxation coefficient was less than 10 %. In contrast, for AFRP and BFRP materials, the million-hour stress relaxation coefficients were between 10 % and 20 %.

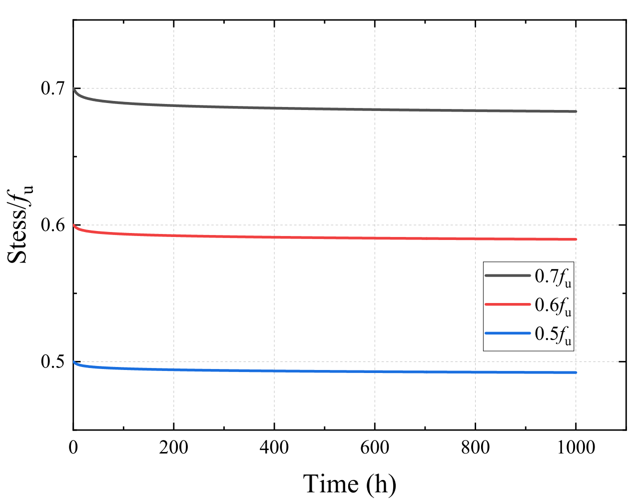

Fig. 13. Stress relaxation curves under different initial stresses.

3.5. *Residual tensile properties*

After the 1000-hour creep test, none of the five specimens underwent creep rupture. To evaluate the residual tensile properties of the cable body and the long-term performance of the anchoring system after the sustained load, an axial tensile test was performed on the specimens. The testing procedure was identical to the short-term tensile test. The failure mode of all specimens was the rupture of the cable body, as shown in Fig. 14, which demonstrated the long-term reliability of the self-anchored anchoring system.

Table 7 presents the residual tensile properties of the self-anchored CFRP cables. The results demonstrated that the specimens subjected to stress levels ranging from 0.3 f_u to 0.6 f_u exhibited tensile strengths greater than their average tensile strength before the creep test. This suggested that straightening uneven fibers increased tensile strength at low or moderate stress levels. Furthermore, the coefficient of variation for the residual tensile strength was less than that for the initial tensile strength, which indicated an improvement in the stability of the CFRP cables. The specimen subjected to a stress level of 0.7 f_u showed the least tensile strength retention (95.13 %), suggesting that the presence of various defects in CFRP, such as voids at the fiber–matrix interface and within the matrix, may have contributed to a reduction in residual tensile strength at high stress levels [26]. Additionally, no significant difference was observed between the residual and initial elastic moduli.

4. Discussion

After studying the creep behavior of CFRP cables, we compared them with traditional steel cables, focusing on performance differences in creep, relaxation, and residual tensile properties. Zhang et al. [35] conducted experiments on a 5-meter-long, 6 mm-diameter steel cable to investigate its creep behavior. The creep strains for steel cables subjected to stress levels of 30 %, 40 %, and 50 % of ultimate strength for 1000 h were 5.68 %, 4.82 %, and 4.09 %, respectively. The creep coefficient of steel cables decreased with an increase in stress level. In contrast, the CFRP cables studied in this paper exhibited creep strains of 4.31 %, 3.37 %, and 3.61 % at the same stress levels, demonstrating lower creep compared to steel cables and superior durability and stability. Additionally, there is no significant correlation between the creep coefficient of CFRP cables and stress levels.

Regarding relaxation performance, Nguyen et al. [36] conducted tests on high-strength steel cables, showing relaxation coefficients of 2.18 %, 2.47 %, and 2.63 % at initial stress levels of 0.5 f_u, 0.6 f_u, and 0.7 f_u, respectively, after 1000 h. Based on the creep curves, this paper derived relaxation coefficients of 1.6 %, 1.8 %, and 2.4 % for the same initial stress levels over 1000 h, indicating lower stress relaxation for the CFRP cables studied here compared to steel cables. Additionally, the relaxation of both steel cables and CFRP cables increased with the rise in

Table 5
Predicted stress retention and relaxation coefficients.

Initial stress level	1000 h		5×10^5 h (57 years)		10^6 h (114 years)	
	Stress retention	Relaxation coefficient	Stress retention	Relaxation coefficient	Stress retention	Relaxation coefficient
0.5 f_u	0.492 f_u	1.6 %	0.484 f_u	3.2 %	0.483 f_u	3.4 %
0.6 f_u	0.589 f_u	1.8 %	0.579 f_u	3.5 %	0.578 f_u	3.7 %
0.7 f_u	0.683 f_u	2.4 %	0.667 f_u	4.7 %	0.665 f_u	5.0 %

Table 6
Comparison of the predicted stress relaxation coefficients.

Study	Material	Calculation formula	Predicted stress relaxation coefficient (10^6 h)
Saadatmanesh et al. (1999) [32]	AFRP	$\psi(t) = 0.0153\ \lg(t) + 0.0227$	11.5 %
Zou (2003) [14]	AFRP	$\psi(t) = 0.00796\ \ln(t) + 0.0147$	12.5 %
Zhu et al. (2006) [33]	AFRP	$\psi(t) = 0.0254\ \lg(t) + 0.0274$	17.9 %
Shi et al. (2017) [25]	BFRP	$\psi(t) = 0.0085\ \ln(t) + 0.007$	12.4 %
Meng et al. (2005) [34]	CFRP	$\psi(t) = 0.0058\ \lg(t) + 0.0131$	4.8 %
Zou (2003) [14]	CFRP	–	≤3%
Saadatmanesh et al. (1999) [30]	CFRP	$\psi(t) = 0.0121\ \lg(t)$-0.0095	6.3 %
The present study	CFRP	–	3.4 %~5%

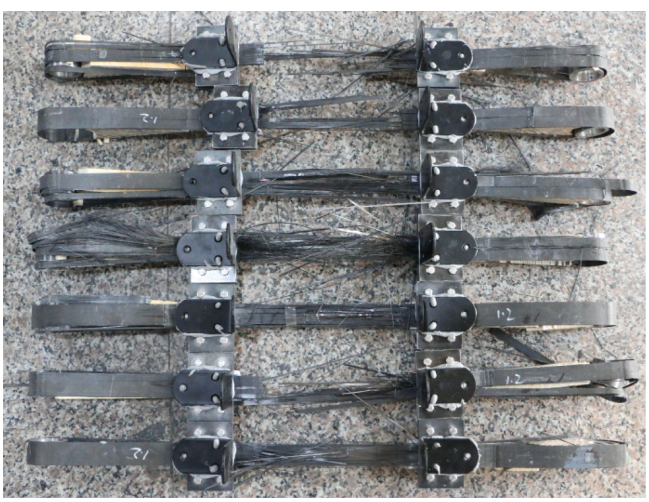

Fig. 14. Failure modes of the CFRP cables.

stress levels.

In terms of residual tensile properties, Nguyen et al.'s study [36] indicated that as the initial stress increased from 0.5 f_u to 0.7 f_u, the elastic modulus of steel cables remained nearly constant, while yield strength and ultimate tensile strength decreased. The CFRP cables studied in this paper exhibited no significant change in elastic modulus under sustained loading. However, at stress levels from 0.3 f_u to 0.6 f_u, the residual tensile strength slightly increased, and at 0.7 f_u stress level, the ultimate tensile strength slightly decreased, indicating better residual tensile properties for the CFRP cables in this study compared to steel cables.

In comparison with steel cables, the CFRP cables studied in this paper showed lower creep and relaxation, and improved residual tensile properties, suggesting that the performance advantages of CFRP have the potential to enhance the stability and reliability of structures, reducing maintenance requirements. However, creep rupture was not observed in this study, and therefore, the creep rupture stress could not be determined. According to relevant literature [37], the creep rupture stress of CFRP cables is reported to be smaller than that of steel cables.

Although CFRP cables have advantages over steel cables in terms of strength, weight, creep, and corrosion resistance, being a new material introduces new challenges that may lead to undesired behavior. In structural engineering, unexpected behavior can pose significant risks. Therefore, any innovation in this area must be thoroughly considered and tested before implementation in civil construction [38]. The poor fire resistance of CFRP cables, apart from anchoring issues, is a major challenge. Due to the polymer matrix of CFRP, it becomes rubbery and viscous at high temperatures, resulting in a decrease in strength and stiffness. Jiang et al. conducted experimental studies on the mechanical properties [39], relaxation [40], and creep [23] of CFRP cables at high temperatures, revealing a 29.8 % decrease in tensile strength and a 35.6 % decrease in elastic modulus at 210 ℃ compared to room temperature. Temperature significantly affects the relaxation and creep properties of CFRP cables. Comparing creep tests of CFRP [23] and steel cables [41] at high temperatures, at 500 ℃, CFRP cables experienced creep rupture at a 0.2 f_u initial stress level within 120 min, while no creep rupture was observed for steel cables under similar conditions, indicating greater sensitivity of CFRP cables to high temperatures. Therefore, appropriate fire prevention measures should be considered in the design of structures using CFRP cables, such as wrapping them with fire-retardant materials [42].

Table 7
Residual tensile properties of the self-anchored CFRP cables.

Specimen	Tensile capacity (kN)	Residual tensile strength (MPa)	Strength retention (%)	Residual elasticity modulus (GPa)	Residual/initial elasticity modulus (%)
0.3 f_u	67.64	2254.54	100.56	137.3	97.89
0.4 f_u	67.84	2261.41	100.87	143.9	102.60
0.5 f_u	72.15	2405.27	107.29	142.6	101.67
0.6 f_u	69.75	2325.11	103.71	135.9	96.89
0.7 f_u	63.98	2132.78	95.13	144.1	102.74
Mean value*	69.35	2311.58	103.11	139.93	99.76
Standard deviation*	1.82	60.69	2.71	3.39	2.42
Coefficient of variation*	2.62 %	2.63 %	2.63 %	2.42 %	2.42 %

*The stress level of 0.7 f_u was excluded from the calculation.

5. Engineering application

The self-anchored CFRP cable has proven to be highly effective in practical engineering due to its lightweight, easy construction process, and excellent resistance to fatigue and long-term creep performance. This success is demonstrated in the construction of a bridge that connects the New Civil Engineering Building and Ho-Sin-Hang Building at Tsinghua University, Beijing, China, as shown in Fig. 15. The 12 m span and 3.5 m height of the bridge consists of steel I-beams, cables, hollow GFRP pultruded profile roof slabs, and ultra-high-performance concrete (UHPC)-FRP hybrid floor slabs. During manufacturing for the sake of convenience, the upper and lower primary beams employed the same section. However, during the bridge operation phase, they bear different loads. The upper primary beam supports the load from the beam's self-weight, hollow GFRP pultruded profile roof slabs, and possible live loads. Meanwhile, the lower primary beam carries the load from the beam's self-weight, UHPC-FRP hybrid floor slabs (which are much heavier than the GFRP pultruded profile roof slabs), wheelchair accessible ramp, stairs, and pedestrian load. Therefore, to maintain equilibrium load distribution, the cables connecting the upper and lower primary beams were introduced. Considering the cable's load-bearing capacity, the bridge's appearance and limited construction conditions, choosing CFRP self-anchored cables for the design was the most logical choice.

The bridge was constructed using a total of sixteen self-anchored CFRP cables, each with a length of 2800 mm and a section dimension of 60 × 10 mm. Due to their lightweight composition of less than 20 kg, the cables were manually installed without the assistance of cranes, as shown in Fig. 16. The installation methodology was meticulously planned and discussed in detail. The CFRP cable has a fixed length, making it challenging to adjust to any potential construction errors. As a result, custom-designed steel fixtures were utilized comprising steel lugs, bolts, nuts, pins, and wedge blocks, as shown in Fig. 16b. The combined application of nuts and bolts enabled the length adjustment of the CFRP cables and the subsequent tensioning. The upper primary beams' bottom flanges were slotted and the steel fixtures were positioned onto the beams (Fig. 15c). Thereafter, the pin was inserted through the steel lug of the steel fixtures and the anchor rings of the CFRP cable to install the cable (Fig. 16d). Due to the CFRP cables' arrangement, some would compress as the bridge loads increased. Consequently, the CFRP cables were pre-tensioned with a tensile strain of approximately 200 με. As limited construction space prevents the use of traditional jacks, pre-tension applications need to be done manually, as shown in Fig. 16e. The workers used a wrench to rotate the nuts, achieving the intended tensile strain. Vibrating wire strain gauges were installed on the CFRP cables, and a real-time signal acquisition system facilitated the control of tensioning and structurcal health monitoring (Fig. 16f).

Fig. 15. The bridge in Tsinghua University.

6. Conclusions

This study investigated the long-term creep performance of the self-anchored CFRP cables subjected to a range of stress levels from 0.3 f_u to 0.7 f_u. In addition to conducting the creep test, axial tensile tests were carried out both prior to and following the creep test. The study delved into the microscopic mechanisms involved in creep phenomena and employed various models to predict the evolution of the creep coefficient. From the test data, the relaxation coefficient was also established, and the influence of creep testing on residual mechanical properties was evaluated. The main findings can be summarized as follows:

(1) The specimens subjected to stress levels from 0.3 f_u to 0.7 f_u exhibited two-stage creep behavior. The first stage showed a rapid increase in creep strain followed by a slowing of the creep rate. The second stage lasted for a longer period, and the creep strain tended to be stable. The principal reasons for the increase in creep strain were the straightening of initial bending fibers and the viscoelastic deformation of the resin.
(2) The Burgers model, Findley model, logarithmic model, and modified logarithmic model were used successfully to fit 1000-hour creep strain curves. However, the Burgers model, Findley model, and modified logarithmic model overestimated the long-term creep development. Utilizing the logarithmic model, we predicted million-hour creep coefficients for CFRP cables, showing a range of 6.1 % to 7.9 % across stress levels from 0.3 f_u to 0.7 f_u.
(3) The stress relaxation curve was derived using the iterative calculation method based on the creep test data. For CFRP cables under initial stress levels that ranged from 0.5 f_u to 0.7 f_u, the predicted million-hour stress relaxation coefficients ranged from 3.4 % to 5.0 %.
(4) The study revealed that holding the load at low and medium stress levels for 1000 h led to an enhancement in both the tensile strength and stability of the CFRP cables. However, at a high stress level of 0.7 f_u, the tensile strength of the CFRP cable decreased by 4.92 %. Additionally, the self-anchored CFRP cables exhibited excellent reliability, as evidenced by the performance of the effective anchorages even after 1000 h of continuous loading.
(5) The 1000-hour creep test did not reveal any significant correlation between the stress level and the creep coefficient, and no creep rupture failure was observed in any of the tested specimens. For future investigations, recommendations include considering higher stress levels and longer creep tests of CFRP cables to gain a more comprehensive understanding of their behavior. Furthermore, exploring the impact of elevated temperatures and fire exposure on CFRP cables is also recommended.
(6) In comparison with steel cable data from the literature, the self-anchored CFRP cables exhibited less creep and relaxation over 1000 h. Steel cables experienced a certain degree of tensile strength reduction after prolonged continuous loading, while CFRP cables, under low to medium stress levels, maintained or even enhanced tensile strength. This was attributed to the straightening of uneven carbon fibers.
(7) The engineering application of self-anchored CFRP cables in the bridge at Tsinghua University was a successful endeavor. The CFRP cables effectively met the requirements of construction convenience, fatigue resistance, and long-term creep performance. Going forward, the utilization of CFRP cables can be implemented in similar situations, such as pedestrian bridges, arch bridges with suspenders, and other comparable scenarios.

CRediT authorship contribution statement

Pengcheng Ai: Conceptualization, Data curation, Formal analysis,

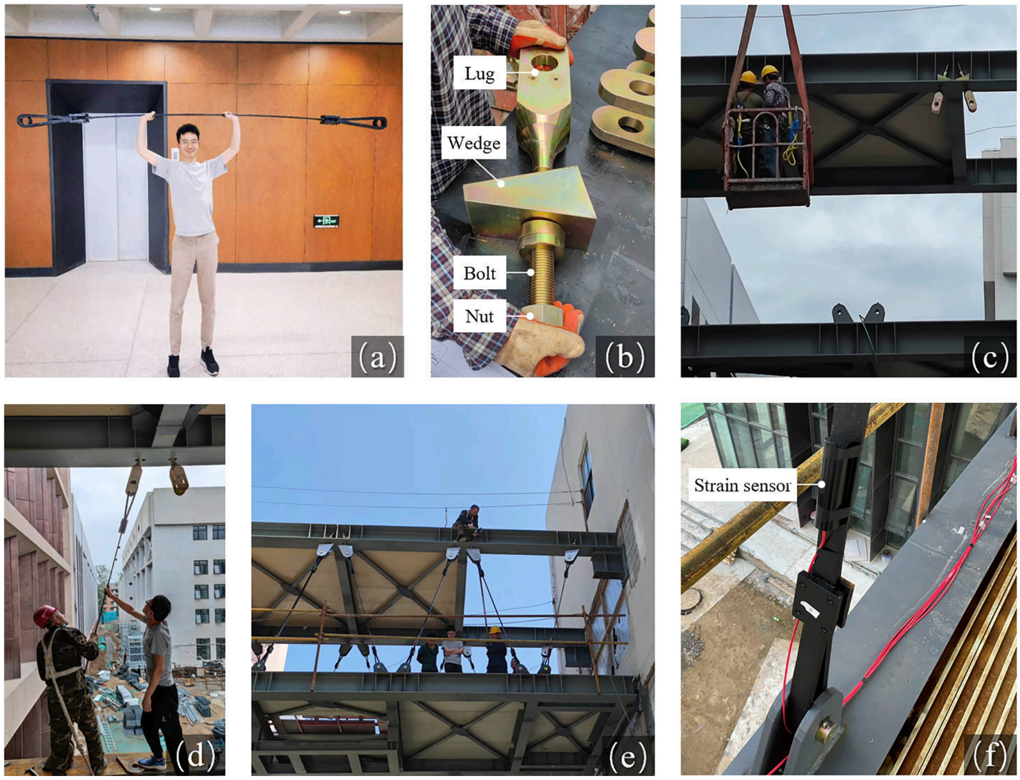

Fig. 16. Installation procedure of the CFRP cables: (a) self-anchored CFRP cable; (b) configuration of steel fixture; (c) installation of steel fixtures; (d) installation of CFRP cables; (e) cable tension monitoring.

Investigation, Methodology, Software, Visualization, Writing – original draft, Writing – review & editing. **Guozhen Ding:** Data curation, Formal analysis, Investigation, Methodology, Visualization, Writing – original draft, Writing – review & editing. **Zhiyuan Li:** Methodology, Writing – review & editing. **Peng Feng:** Conceptualization, Funding acquisition, Project administration, Resources, Supervision, Validation, Writing – review & editing.

Declaration of competing interest

The authors declare that they have no known competing financial interests or personal relationships that could have appeared to influence the work reported in this paper.

Data availability

Data will be made available on request.

Acknowledgments

This research was supported by the National Key R&D Program of China (2022YFC3801800), the National Natural Science Foundation of China (U2106219, 52208264), grants from the Institute for Guo Qiang, Tsinghua University (2020GQG1002), and the support by XPLORER PRIZE from New Cornerstone Science Foundation.

References

[1] Meier U. Carbon fiber reinforced polymer cables: why? why not? what if? Arab J Sci Eng 2012;37(2):399–411.
[2] Ai P, Feng P, Lin H, Zhu P, Ding G. Novel self-anchored CFRP cable system: Concept and anchorage behavior. Compos Struct 2021;263.
[3] Ding G, Feng P, Wang Yu, Ai P. Novel pre-clamp lap joint for CFRP plates: design and experimental study. Compos Struct 2022;302:116240.
[4] Feng P, Dong L, Ding G, Zou Y, Shi W. Engineering application of self-anchored integrated CFRP cables. Proceedings of IABSE Congress Nanjing 2022.
[5] Liu Y, Zwingmann B, Schlaich M. Carbon fiber reinforced polymer for cable structures—a review. Polymers 2015;7:2078–99.
[6] Wang L, Zhang J, Xu J, Han Q. Anchorage systems of CFRP cables in cable structures—a review. Constr Build Mater 2018;160:82–99.
[7] Ding G, Feng P, Wang Yu, Ai P, Wang Q. Long-term bolt preload relaxation and contact pressure distribution in clamping anchorages for CFRP plates. Compos Struct 2024;329.
[8] Hu L, Li W, Feng P. Long-term behavior of CFRP plates under sustained loads. Adv Struct Eng 2022;25(5):939–53.
[9] Zhao J, Mei K, Wu J. Long-term mechanical properties of FRP tendon–anchor systems — a review. Constr Build Mater 2020;230.
[10] Ascione F, Berardi VP, Feo L, Giordano A. An experimental study on the long-term behavior of CFRP pultruded laminates suitable to concrete structures rehabilitation. Compos B Eng 2008;39(7-8):1147–50.
[11] Rossini M, Saqan E, Nanni A. Prediction of the creep rupture strength of GFRP bars. Constr Build Mater 2019;227.
[12] ASTM D7337. Standard test method for tensile creep rupture of Fiber Reinforced Polymer matrix. vol. 12, West Conshohocken, PA: ASTM International; 2019, p. 1–6.
[13] Guimarães GB, Burgoyne CJ. Creep behaviour of a parallel-lay aramid rope. J Mater Sci 1992;27(9):2473–89.
[14] Zou PXW. Long-term properties and transfer length of fiber-reinforced polymers. J Compos Constr 2003;7(1):10–9.
[15] Banibayat P, Patnaik A. Creep rupture performance of basalt fiber-reinforced polymer bars. J Aerosp Eng 2015;28(3).
[16] Ascione L, Berardi VP, Aponte D. Creep phenomena in FRP materials. Mech Res Commun 2012;43:15–21.
[17] Ascione L, Berardi VP, D'Aponte A. A viscoelastic constitutive law for FRP materials. International Journal of Computational Methods in Engineering Science and Mechanics 2011;12(5):225–32.
[18] Wang X, Shi J, Liu J, Yang L, Wu Z. Creep behavior of basalt fiber reinforced polymer tendons for prestressing application. Mater Des 2014;59:558–64.
[19] Wang X, Shi J, Wu Z, Zhu Z. Creep strain control by pretension for basalt fiber-reinforced polymer tendon in civil applications. Mater Des 2016;89:1270–7.
[20] Benmokrane B, Brown VL, Mohamed K, Nanni A, Rossini M, Shield C. Creep-rupture limit for GFRP bars subjected to sustained loads. Journal of Composites for Construction. 2019; 23:6019001.
[21] Yang X, Arockiasamy M, Mirmiran A, Potter W. High creep stress test of carbon fiber – composite cable with generic field-made anchorage. J Compos Constr 2017; 21:6017001.
[22] Yang D, Zhang J, Song S, Zhou F, Wang C. Experimental investigation on the creep property of carbon fiber reinforced polymer tendons under high stress levels. Materials 2018;11:2273.

[23] Jiang Z, Fang Z, Fang C, Li Q, Wang Z. Experimental investigation on high-temperature creep behavior of carbon fiber reinforced polymer cable. Compos Struct 2022;291.
[24] JSCE-E 533. Test method for creep failure of continuous fiber reinforcing materials, Japan Society of Civil Engineers; 2004.
[25] Shi J, Wang X, Huang H, Wu Z. Relaxation behavior of prestressing basalt fiber-reinforced polymer tendons considering anchorage slippage. J Compos Mater 2017;51(9):1275–84.
[26] Shi J, Wang X, Wu Z, Zhu Z. Creep behavior enhancement of a basalt fiber-reinforced polymer tendon. Constr Build Mater 2015;94:750–7.
[27] Findley WN. Mechanism and mechanics of creep of plastics. SPE J 1960;16:57–65.
[28] Dutta PK, Hui D. Creep rupture of a GFRP composite at elevated temperatures. Comput Struct 2000;76(1–3):153–61.
[29] Tamuzs V, Maksimovs R, Modniks J. Long-term creep of hybrid FRP bars. Proceedings of the fifth international conference on fibre-reinforced plastics for reinforced concrete structures, Cambridge, UK. 2001. Thomas Telford Publishing.
[30] Saadatmanesh H, Tannous FE. Relaxation, creep, and fatigue behavior of carbon fiber reinforced plastic tendons. Materials Journal 1999;96(2):143–53.
[31] Lakes RS, Vanderby R. Interrelation of creep and relaxation: a modeling approach for ligaments. 1999.
[32] Saadatmanesh H, Tannous FE. Long-term behavior of aramid fiber reinforced plastic (ARFP) tendons. Materials Journal. 1999; 96(3):297-305.
[33] Zhu H, Lv Z, Zhang J, Tang H, Gao H. Experimental study of relaxation performance of AFRP tendons. Industrial Construction 2006;36:62–4. In Chinese.
[34] Meng L, Xu F, Guan J, Zhai Q, Lin X. Experiment study on relaxation losses of CFRP tendons. Construction Technology 2005;34:40–1. In Chinese.
[35] Zhang W, Yuan X, Yang L, Deng M. Research on creep constitutive model of steel cables. Constr Build Mater 2020;246.
[36] Nguyen N-V, Vu Q-A, Kim S-E. An experimental study on stress relaxation behaviour of high strength steel wire: microstructural evolution and degradation of mechanical properties. Constr Build Mater 2020;261.
[37] Yang Y, Fahmy MFM, Guan S, Pan Z, Zhan Y, Zhao T. Properties and applications of FRP cable on long-span cable-supported bridges: a review. Compos B Eng 2020;190.
[38] Foraboschi P, Others. Appunti per una inedita epistemologia dell'ingegneria strutturale= Suggestions for a New Epistemology of Structural Engineering. VESPER. 2023; 8:154-68.
[39] Jiang Z, Fang Z, Fang C, Li Q, Wang Z. Mechanical properties under high-temperature and fire resistant limit of carbon fiber reinforced polymer cable. Constr Build Mater 2022;361.
[40] Jiang Z, Lv R, Fang Z, Li Q, Fang C, Wang Z. Experimental study on high-temperature relaxation behavior of carbon fiber reinforced polymer cable. Constr Build Mater 2022;330.
[41] Du Y, Wu Y, Umar AM, Zhu S. Elevated temperature creep model of parallel wire strands. Front Struct Civ Eng 2023;17(7):1060–71.
[42] Zhuge P, Tao G, Wang B, Jie Z, Zhang Z. Effects of high temperatures on the performance of carbon fiber reinforced polymer (CFRP) composite cables protected with fire-retardant materials. Materials 2022;15(13):4696.